Hindawi
International Journal of Photoenergy
Volume 2017, Article ID 7284367, 6 pages
https://doi.org/10.1155/2017/7284367

Research Article

Tandem Solar Cells Based on Cu_2O and c-Si Subcells in Parallel Configuration: Numerical Simulation

Mihai Răzvan Mitroi,[1] Valerică Ninulescu,[1] and Laurenţiu Fara[1,2]

[1]*University POLITEHNICA of Bucharest, 313 Splaiul Independentei, 060042 Bucharest, Romania*
[2]*Academy of Romanian Scientists, 54 Splaiul Independentei, 050094 Bucharest, Romania*

Correspondence should be addressed to Valerică Ninulescu; ninulescu.valerica@gmail.com

Received 24 April 2017; Revised 16 June 2017; Accepted 6 July 2017; Published 8 August 2017

Academic Editor: Christin David

A tandem solar cell consisting of a bottom c-Si high-efficiency subcell and a top low-cost Cu_2O subcell in parallel configuration is evaluated for the first time by a use of an electrical model. A numerical simulation based on the single-diode model of the solar cell is performed. The numerical method determines both the model parameters and the parameters of the subcells and tandem from the maximization of output power. The simulations indicate a theoretical limit value of the tandem power conversion efficiency of 31.23% at 298 K. The influence of temperature on the maximum output power is analyzed. This tandem configuration allows a great potential for the development of a new generation of low-cost high-efficiency solar cells.

1. Introduction

Recently, tandem solar cells made up of various materials such as silicon (monocrystalline, polycrystalline, and amorphous) [1–3], perovskite [4–6], polymer [7, 8], dye-sensitized solar cells [9], and quantum dot solar cells [10] have been theoretically or experimentally studied. However, tandems with a high efficiency at low cost have still not been realized. The silicon-based tandem heterojunction solar cells made up of a high-efficiency crystalline silicon (c-Si) bottom subcell and a low-cost upper subcell are a promising candidate for both reducing the fabrication costs and increasing the efficiency above the silicon single-junction record of 25.6% [11]. The band gap of the top subcell is required to be higher than the band gap of silicon (1.1 eV) in order to absorb the photons of higher energy, thus yielding two complementary absorbing subcells. Generally, the bottom subcell generates a higher current and has a lower open-circuit voltage than the top subcell.

The cuprous oxide (Cu_2O) solar cell represents one of the best choices as top subcell. This semiconducting metal oxide has a band gap of 2.1 eV, a high optical absorption, is nontoxic, and has the potential of a low manufacturing cost [12]. The theoretical limit of the power conversion efficiency for a Cu_2O solar cell is approximately 20% [13, 14] under the solar radiation spectrum AM 1.5G. However, the highest conversion efficiency of 81% achieved experimentally for a solar cell made up of zinc oxide (ZnO) and Cu_2O based on thermally oxidized copper sheets [15] suggests the potential of further increase of the conversion efficiency.

In this paper, a comprehensive numerical simulation of the performance parameters of a tandem solar cell based on c-Si and Cu_2O subcells in parallel configuration is presented. The ideal working conditions for tandem are defined. The single-diode model for solar cells is used [16]. The parameters of the subcells and tandem are calculated from the maximum condition of the output power. The values of the main parameters, that is, the short-circuit current density (J_{sc}), the open-circuit voltage (V_{oc}), the fill factor (FF), and the power conversion efficiency (η), are calculated and discussed. The value of the maximum power conversion efficiency of this configuration type is estimated. The influence of temperature (T) on the performance of the tandem is analyzed.

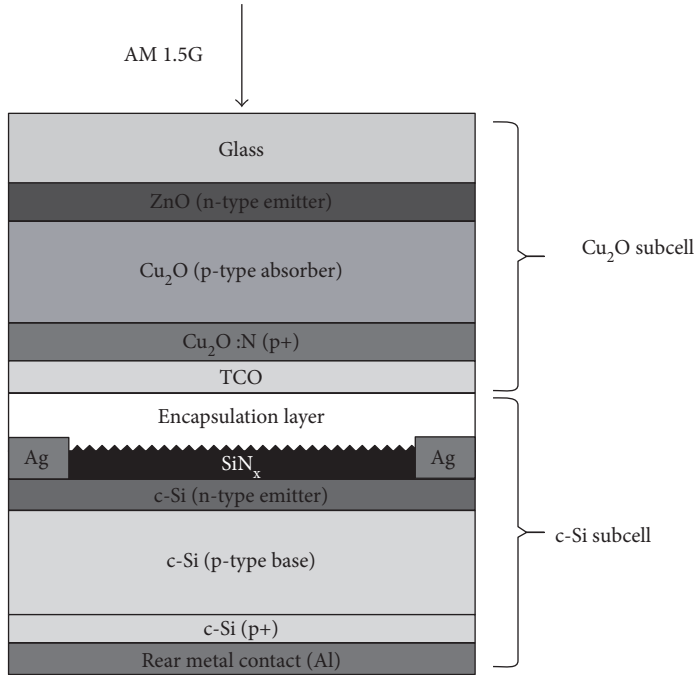

Figure 1: Schematic configuration design of a tandem solar cell based on Cu_2O and c-Si subcells.

All the programs used for the simulations are written in Mathcad environment.

2. Theoretical Model

A tandem solar cell based on a bottom c-Si subcell and a top Cu_2O subcell as active layers of p-type materials is investigated. For the Cu_2O subcell, a wide range of possible n-type materials, including ZnO, ZnS, TiO_2, CdS, and Ga_2O_3 [13–15] can be used. There are two possibilities of electrical connection for the two subcells, namely, series and parallel. The parallel connection is more advantageous [17] since it does not require current matching between the subcells and allows independent optimization of the subcells. A four-terminal device has the subcells electrically decoupled and independently controllable that can be connected in parallel, ensuring a maximum output power at all times [18]. The tandem efficiency is estimated to reach values above 30% [1, 2, 6, 19]. A possible four-terminal configuration is presented in Figure 1 [20].

The following ideal conditions of the solar cell operation—including illumination conditions, subcell materials, radiation absorption processes, and carrier generation processes in subcells—are considered:

(1) the solar radiation spectrum AM 1.5G [21];

(2) no optical losses due to nonactive layers (glass, n-type materials, encapsulation layer, etc.);

(3) the carrier-injection efficiency $\eta_{inj} = 1$ for each subcell;

(4) no resistive and recombination losses, $R_s = 0$, for each subcell;

(5) the standard temperature $T^* = 298$ K.

2.1. Optical Model. In the conditions above, the photoelectron generation rate determined by the solar radiation incident on the surface of the active layer is

$$G_{inj}(L) = \int_{\lambda_1}^{\lambda_2} \alpha(\lambda)\phi(\lambda)\exp[-\alpha(\lambda)L]d\lambda, \quad (1)$$

where L is the thickness of the active layer (Cu_2O or c-Si), λ is the wavelength of incident radiation, the integration limits λ_1 and λ_2 are imposed by the absorption characteristics of the active layer through the absorption coefficient $\alpha(\lambda)$, and $\phi(\lambda)$ is the spectral incident photon flux density. The photoelectrons are then collected without any losses.

Note that there is a range of wavelengths in which both Cu_2O and c-Si absorb radiation. The incident radiation on the top surface of the Cu_2O layer is the entire AM 1.5G solar spectrum; at the top of the c-Si layer, the spectral irradiance of the AM 1.5G solar spectrum is diminished due to the partial absorption of Cu_2O layer. These lead to the possibility of optimization in choosing the thickness of the two layers so that the output power of tandem cell is at maximum.

2.2. Electrical Model. The current density J through each subcell, in the single-diode model [16], is

$$J = J_L - J_0\left[\exp\left(\frac{V + R_s J}{\gamma V_{th}}\right) - 1\right] - \frac{V + R_s J}{R_{sh}}, \quad (2)$$

where J_L is the light-generated current density, J_0 is the reverse saturation current density of the diode, V is the

output voltage, γ is the ideality factor, R_s is the series resistance, R_{sh} is the shunt resistance, and $V_{th} = k_B T/q$ is the thermal voltage, where k_B and q denote the Boltzmann constant and elementary electric charge, respectively. In the conditions above, (2) becomes

$$J_{ideal} = J_L - J_0 \left[\exp\left(\frac{V}{\gamma V_{th}}\right) - 1\right] - \frac{V}{R_{sh}}. \quad (3)$$

In the approximation of a negligible diffusion of carriers and assuming a uniform field across the active layer (subcell materials are without any defects and impurities), the light-generated current density is [22]

$$J_L = qG_{inj}(L)\mu\tau \frac{V_{bi} - V}{L}\left\{1 - \exp\left[-\frac{L^2}{\mu\tau(V_{bi} - V)}\right]\right\}, \quad (4)$$

where V_{bi} is the built-in voltage [23] and the product $\mu\tau$ is given by the relation

$$\mu\tau = \mu_p\tau_p + \mu_n\tau_n, \quad (5)$$

where μ_p, μ_n and τ_p, τ_n are the hole and electron mobilities and lifetimes, respectively.

By use of (3) and (4), the output power density of the solar cell is

$$P = \left\{qG_{inj}(L)\mu\tau \frac{V_{bi} - V}{L}\left[1 - \exp\left(-\frac{L^2}{\mu\tau(V_{bi} - V)}\right)\right] - J_0\left[\exp\left(\frac{V}{\gamma V_{th}}\right) - 1\right] - \frac{V}{R_{sh}}\right\}V. \quad (6)$$

One can observe that, at a given temperature, P depends on seven parameters: L, J_0, V, R_{sh}, γ, $\mu\tau$, and V_{bi}.

In the following, the two subcells will be considered electrically connected in parallel. In the steady state, the current densities and voltages obey the relations

$$J_{tandem} = J_{top} + J_{bottom} \quad (7)$$

and

$$V_{tandem} = V_{top} = V_{bottom}. \quad (8)$$

2.3. The Influence of Temperature on Tandem Cell Performance. The solar cells for usual applications are used at temperatures ranging from −15°C to 100°C. Many studies have pointed out that the performance of solar cells degrades as temperature increases [24–28]. The variation of R_{sh} with temperature slightly affects the efficiency of a solar cell [27, 28]. We analyze the variation with temperature of parameters V_{th} and J_0.

The thermal voltage dependence on temperature is

$$V_{th}(T) = \frac{k_B T}{q} = V_{th}^* \frac{T}{T^*}, \quad (9)$$

where V_{th}^* is the thermal voltage for the standard temperature.

The dependence on temperature of the reverse bias saturation current density J_0 is [25]

Table 1: Single-diode model parameter values of the Cu_2O and c-Si ideal cells.

Cell	R_{sh} (Ω cm^2)	γ	J_0 (pA/cm^2)	$\mu\tau$ (cm^2/V)	V_{bi} (V)
Cu_2O	5000	3.00	1.0	$5.00 \cdot 10^{-5}$	1.91
c-Si	6500	1.68	2.3	$1.55 \cdot 10^{-2}$	1.16

Table 2: Cell parameters calculated for the values from Table 1.

Cell	J_{sc} (mA/cm^2)	V_{oc} (V)	FF (%)	η (%)
Cu_2O	13.38	1.835	78.51	19.29
c-Si	37.76	1.014	81.70	31.29

$$J_0(T) = J_0^*\left(\frac{T}{T^*}\right)^3 \exp\left[\frac{E_g(T)}{k_B}\left(\frac{1}{T^*} - \frac{1}{T}\right)\right], \quad (10)$$

where $J_0^* = J_0|_{T=T^*}$ and $E_g(T)$ is the band gap energy of the semiconductor (the active layer) which depends on temperature by the relationship [26]

$$E_g(T) = E_g(0) - \frac{\alpha T^2}{T + \beta}, \quad (11)$$

where $E_g(0)$ is the band gap value at $T \approx 0$ K, and α and β are constants.

3. Results and Discussion

The operation of a tandem solar cell with a Cu_2O top subcell and a c-Si bottom subcell is simulated using the presented theoretical model. The performance of the tandem is obtained by numerical simulations in the conditions stated in Section 2. The solar radiation spectrum AM 1.5G has values between the wavelength limits 280 nm and 4000 nm and a flux power density of 1000 W/m^2. The active layers of c-Si and Cu_2O have the absorption wavelength range ([280 nm, 1450 nm] [29] and [280 nm, 640 nm] [30], resp.).

The parameters R_{sh}, γ, J_0, $\mu\tau$, and V_{bi} of the single-diode model are material constants that depend on materials and the manufacturing of cells. Therefore, the calculated parameters of the c-Si and Cu_2O cells remain unchanged in the tandem configuration. These parameters can be calculated by different methods, such as fitting methods [31, 32], Lambert-W function [33], and asymptotic approximation [34] by use of J–V experimental data.

The method used in this paper was previously applied to the study of solar cells containing a heterojunction with Cu_2O [14]. The method consists in the maximization of the output power density (7) which leads to the parameter values of the theoretical model. The obtained values, separately for the Cu_2O and c-Si cells, are presented in Table 1. The cell voltages are 1.61 V and 0.88 V, respectively, and the thickness of the active layers is 11.94 μm and 115.00 μm, respectively. The cell parameters calculated based on the values of Table 1 are shown in Table 2. The results indicate a maximum power conversion efficiency of 19.29% for the Cu_2O cell of 11.94 μm active layer thickness and 31.29% for the c-Si cell of 115.00 μm active layer thickness. The maximum

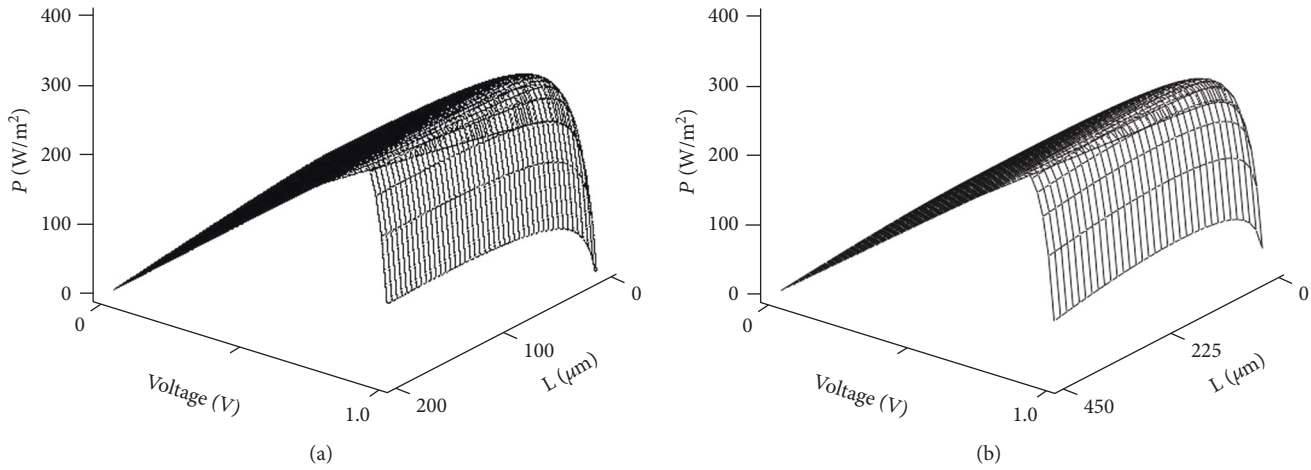

Figure 2: The output power density of a tandem cell versus voltage and the total thickness of the active layers for two ratios of subcell thickness: (a) $L_{Cu_2O}/L_{c\text{-}Si} = 1/40$ and (b) $L_{Cu_2O}/L_{c\text{-}Si} = 1/100$.

Table 3: The parameter values of the Cu_2O and c-Si subcells and the tandem in the case of maximum output power density of the tandem cell.

Cell	L (μm)	J_{sc} (mA/cm^2)	V_{oc} (V)	FF (%)	η (%)
Cu_2O top subcell	0.64	10.19	—	—	8.78
c-Si bottom subcell	60.62	27.34	—	—	22.45
Tandem cell	—	37.53	1.015	82.02	31.23

values of the power conversion efficiency are in good agreement with the data reported in literature, ~20% for the Cu_2O cell [13, 14] and 32.9% [35], 29.8% [36], or 33.5% [5] for the c-Si cell.

The dependence of the tandem output power density, (6) where J_{ideal} is J_{tandem}, on the voltage and the total thickness of the active layers (Cu_2O and c-Si layers) is analyzed. The results for two ratios of the thicknesses of the active layers, $L_{Cu_2O}/L_{c\text{-}Si} = 1/40$ and $L_{Cu_2O}/L_{c\text{-}Si} = 1/100$, are shown in Figure 2. They show a maximum of the tandem output power density. The output power density of tandem as a function of voltage, and the thickness of the two active layers L_{Cu_2O} and $L_{c\text{-}Si}$ has been maximized. The calculated parameters for the two subcells and tandem are presented in Table 3. The obtained maximum output power density is 312.3 W/m^2 for 0.88 V tandem voltage, 0.64 μm Cu_2O layer thickness, and 60.62 μm c-Si thickness. Therefore, the maximum power conversion efficiency is 31.23%. It can be noticed that in case of tandem, the thickness of the subcells is significantly reduced compared to the case of separate cells (see Table 2). In case of the c-Si and Cu_2O layer thicknesses obtained above, the J–V curves for the two subcells, as well as for the tandem cell, are presented in Figure 3. The open-circuit voltage of the tandem cell (see Table 3) is located between the V_{oc} values of separate subcells (see Table 2), practically being equal to that of the separate c-Si subcell. There is a limitation in the voltage for tandem operation, but this drawback is compensated by the advantages of

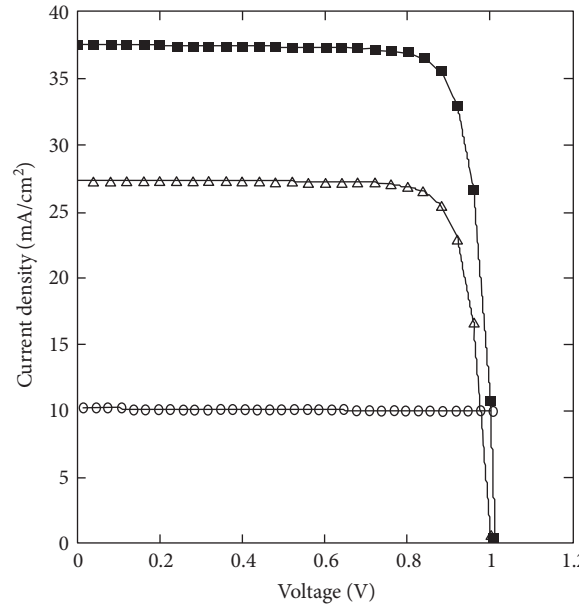

Figure 3: Current density versus voltage for the two subcells in tandem and tandem cell, for the thicknesses 0.64 μm and 60.62 μm of the Cu_2O layer and the c-Si layer, respectively: J_{Cu_2O} (○), $J_{c\text{–}Si}$ (Δ), and J_{tandem} (■).

parallel connection [18]. These results are consistent with theoretical or experimental values reported in literature for other types of tandem cells [5, 7, 8, 37].

Figure 4 shows the dependence of the maximum output power density on temperature for the thickness of active layers from Table 3 and for the following parameter values of (11): $E_{g,Cu_2O}(0) = 2.173$ eV, $\alpha_{Cu_2O} = 4.8 \cdot 10^{-4}$ eV/K, $\beta_{Cu_2O} = 275$ K [38], $E_{g,c\text{-}Si}(0) = 1.1557$ eV, $\alpha_{c\text{-}Si} = 7.021 \cdot 10^{-4}$ eV/K, and $\beta_{c\text{-}Si} = 1108$ K [26]. A decrease of the maximum output power density with increasing temperature is observed. This decrease is due to the temperature dependence of the reverse bias saturation current density (10). The drop

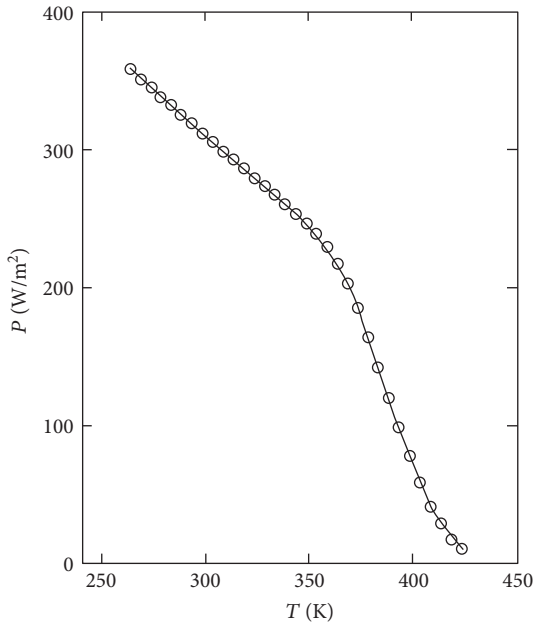

Figure 4: The maximum output power density of the tandem cell versus temperature, for the thicknesses 0.64 μm and 60.62 μm of Cu_2O layer and c-Si layer, respectively.

of the output power density is 20.90% for a temperature increase from 298 K to 348 K. This result indicates that the temperature is a major factor in decreasing the tandem solar cell performance.

4. Summary and Concluding Remarks

The paper presents a comprehensive numerical simulation of performance optimization of the tandem solar cells using c-Si and Cu_2O subcells. A numerical simulation based on the single-diode model of the solar cell is performed. The numerical method determines both the model parameters and the parameters of the subcells and tandem.

The thickness of active layers c-Si and Cu_2O in tandem cell is obtained from the maximization of output power. The tandem power conversion efficiency has a maximum of 31.23% for a 0.64 μm Cu_2O layer thickness and 60.62 μm c-Si layer thickness. These thicknesses are significantly reduced compared to the case of separate cells, and the efficiency represents the theoretical limit at 298 K. A realistic model of the tandem will include optical losses for each layer of the tandem as well as a smaller than unity injection efficiency in the active layers. Therefore, a lower value of the tandem efficiency is expected. The numerical simulation shows that temperature is a factor in decreasing tandem cell performance; therefore, temperature should be taken into account in tandem design.

The results of this paper give indications for the design and performance optimization of real tandem solar cells using Cu_2O and c-Si subcells.

An approach of the solar cell tandem using experimental data will be the subject of future research.

Conflicts of Interest

The authors declare that there is no conflict of interest regarding the publication of this paper.

Acknowledgments

This work was supported by (1) the project MultiscaleSolar MP1406, 2015–2019, supported by the European Commission through COST program (the article processing charges), and (2) the project SOLHET, 2016–2019, M-ERA.Net program, supported by the Research Council of Norway (RCN) and the Romanian Executive Agency for Higher Education, Research, Development and Innovation Funding (UEFISCDI).

References

[1] T. P. White, N. N. Lal, and K. R. Catchpole, "Tandem solar cells based on high-efficiency c-Si bottom cells: top cell requirements for >30% efficiency," *IEEE Journal of Photovoltaics*, vol. 4, no. 1, pp. 208–214, 2014.

[2] C. Ulbrich, C. Zahren, A. Gerber et al., "Matching of silicon thin-film tandem solar cells for maximum power output," *International Journal of Photoenergy*, vol. 2013, Article ID 314097, 7 pages, 2013.

[3] M. Taguchi, A. Yano, S. Tohoda et al., "24.7% record efficiency HIT solar cell on thin silicon wafer," *IEEE Journal of Photovoltaics*, vol. 4, pp. 96–99, 2014.

[4] P. Löper, S.-J. Moon, S. M. d. Nicolas et al., "Organic–inorganic halide perovskite/crystalline silicon four-terminal tandem solar cells," *Physical Chemistry Chemical Physics*, vol. 17, p. 1619, 2015.

[5] H. M. Futscher and B. Ehrler, "Efficiency limit of perovskite/Si tandem solar cells," *ACS Energy Letters*, vol. 1, no. 4, pp. 863–868, 2016.

[6] R. Asadpour, R. V. K. Chavali, M. R. Khan, and M. A. Alam, "Bifacial Si heterojunction-perovskite organic-inorganic tandem to produce highly efficient (η T*~ 33%) solar cell," *Applied Physics Letters*, vol. 106, article 243902, 2015.

[7] A. Hadipour, B. d. Boer, and P. W. M. Blom, "Device operation of organic tandem solar cells," *Organic Electronics*, vol. 9, pp. 617–624, 2008.

[8] L. Yang, H. Zhou, S. C. Price, and W. You, "Parallel-like bulk heterojunction polymer solar cells," *Journal of the American Chemical Society*, vol. 134, pp. 5432–5435, 2012.

[9] A. K. Baranwal, T. Shiki, Y. Ogomi, S. S. Pandey, T. Ma, and S. Hayase, "Tandem dye-sensitized solar cells with a back-contact bottom electrode without a transparent conductive layer," *RSC Advances*, vol. 4, pp. 47735–47742, 2014.

[10] S. Diao, X. Zhang, Z. Shao, K. Ding, J. Jie, and X. Zhang, "12.35% efficient graphene quantum dots/silicon heterojunction solar cells using graphene transparent electrode," *Nano Energy*, vol. 31, pp. 359–366, 2017.

[11] K. Masuko, M. Shigematsu, T. Hashiguchi et al., "Achievement of more than 25% conversion efficiency with crystalline silicon heterojunction solar cell," *IEEE Journal of Photovoltaics*, vol. 4, pp. 1433–1435, 2014.

[12] B. K. Meyer, A. Polity, D. Reppin et al., "The physics of copper oxide (Cu_2O)," *Chapter 6: Semiconductors and Semimetals*, vol. 88, pp. 201–226, 2013.

[13] Y. Takiguchi and S. Miyajima, "Device simulation of cuprous oxide heterojunction solar cells," *Japanese Journal of Applied Physics*, vol. 54, no. 11, article 112303, 2015.

[14] M. R. Mitroi, V. Ninulescu, and L. Fara, "Performance optimization of solar cells based on heterojunctions with Cu_2O–numerical analysis," *Journal of Energy Engineering*, pp. 1943–7897, 2017.

[15] T. Minami, Y. Nishi, and T. Miyata, "Efficiency enhancement using a $Zn_{1-x}Ge_x$-O thin film as an n-type window layer in Cu_2O–based heterojunction solar cells," *Applied Physics Express*, vol. 9, article 052301, 2016.

[16] K. Ishibashi, Y. Kimura, and M. Niwano, "An extensively valid and stable method for derivation of all parameters of a solar cell from a single current-voltage characteristic," *Journal of Applied Physics*, vol. 103, article 094507, 2008.

[17] Y. Hamakawa, Ed., *Thin-Film Solar Cells: Next Generation Photovoltaics and Its Applications*, Berlin, Springer, 2004.

[18] S. Reynolds and V. Smirnov, "Modelling performance of two- and four-terminal thin-film silicon tandem solar cells under varying spectral conditions," *Energy Procedia*, vol. 84, pp. 251–260, 2015.

[19] R. E. Brandt, M. Young, H. H. Park et al., "Band offsets of n-type electron-selective contacts on cuprous oxide (Cu_2O) for photovoltaics," *Applied Physics Letters*, vol. 105, no. 26, article 263901, 2014.

[20] Ø. Nordseth, R. Kumar, K. Bergum et al., "Optical analysis of a ZnO/Cu_2O subcell in a silicon-based tandem heterojunction solar cell," *Green and Sustainable Chemistry*, vol. 7, pp. 57–69, 2017.

[21] ASTM G173-03, "Reference spectra derived from SMARTS v. 2.9.2," 2012, March, 2017, http://rredc.nrel.gov/solar/spectra/am1.5/ASTMG173/ASTMG173.html.

[22] T. Aernouts, *Organic Bulk Heterojunction Solar Cells: From Single Cell towards Fully Flexible Photovoltaic Module, [Ph.D. Thesis]*, Departement Natuurkunde, Faculteit Wetenschappen, Katholieke Universiteit Leuven, Belgium, 2006, March 2017, https://lirias.kuleuven.be/bitstream/1979/402/5/PhD.

[23] X. Chao, Y. Ruo-He, and G. Kui-Wei, "Photovoltage analysis of a heterojunction solar cell," *Chinese Physics B*, vol. 20, no. 5, article 057302, 2011.

[24] M. Abderrezek, M. Fathi, S. Mekhilef, and F. Djahli, "Effect of temperature on the GaInP/GaAs tandem solar cell performances," *International Journal of Renewable and Sustainable Energy*, vol. 5, no. 2, pp. 629–634, 2015.

[25] P. Singh and N. M. Ravindra, "Temperature dependence of solar cell performance–an analysis," *Solar Energy Materials and Solar Cells*, vol. 101, pp. 36–45, 2012.

[26] Y. P. Varshni, "Temperature dependence of the energy gap in semiconductors," *Physica*, vol. 34, pp. 149–154, 1967.

[27] F. Attivissimo, A. D. Nisio, M. Savino, and M. Spadavecchia, "Uncertainty analysis in photovoltaic cell parameter estimation," *IEEE Transactions on Instrumentation and Measurement*, vol. 61, no. 5, pp. 1334–1342, 2012.

[28] P. Singh, S. N. Singh, and M. LalM. Husain, "Temperature dependence of *I–V* characteristics and performance parameters of silicon solar cell," *Solar Energy Materials and Solar Cells*, vol. 92, pp. 1611–1616, 2008.

[29] M. A. Green, "Self-consistent optical parameters of intrinsic silicon at 300K including temperature coefficients," *Solar Energy Materials and Solar Cells*, vol. 92, no. 11, pp. 1305–1310, 2008.

[30] C. Malerba, F. Biccari, C. L. A. Ricardo, M. D'Incau, P. Scardi, and A. Mittiga, "Absorption coefficient of bulk and thin film Cu_2O," *Solar Energy Materials and Solar Cells*, vol. 95, no. 10, pp. 2848–2854, 2011.

[31] M. R. Mitroi, V. Iancu, L. Fara, and M. L. Ciurea, "Numerical analysis of *J–V* characteristics of a polymer solar cell," *Progress in Photovoltaics: Research and Applications*, vol. 19, no. 3, pp. 253–377, 2011.

[32] R. S. AbdelHady, "Detecting the parameters of solar cells using efficient curve fitting techniques," *International Journal of Engineering Research and Technology*, vol. 7, no. 3, pp. 185–199, 2014.

[33] J. Cubas, S. Pindado, and C. d. Manuel, "Explicit expressions for solar panel equivalent circuit parameters based on analytical formulation and the Lambert *W*-function," *Energies*, vol. 7, pp. 4098–4115, 2014.

[34] A. Bărar, D. Mănăilă-Maximean, O. Dănilă, and M. Vlădescu, "Parameter extraction of an organic solar cell using asymptotic estimation and Lambert W function," in *Proceedings SPIE 10010, Advanced Topics in Optoelectronics, Microelectronics, and Nanotechnologies VIII*, Article ID 1001034, 2016.

[35] R. Matson, R. Bird, and K. Emery, "Terrestrial solar spectra, solar simulation and solar cell efficiency measurement," Tech. Rept. SERI/TR-612-964: DE82002082, U.S. Department of Energy, ON, 1981.

[36] T. Tiedje, E. Yablonovitch, G. D. Cody, and B. G. Brooks, "Limiting efficiency of silicon solar cells," *IEEE Transactions on Electron Devices*, vol. ED-31, no. 5, 1984.

[37] D. Zhanga, W. Soppea, and R. E. I. Schroppa, "Design of 4-terminal solar modules combining thin-film wide-bandgap top cells and c-Si bottom cells," *Energy Procedia*, vol. 77, pp. 500–507, 2015.

[38] F. Biccari, *Defects and Doping in Cu_2O, [Ph.D. Thesis]*, Universita di Roma, Italia, 2009, March 2017, http://www.phys.uniroma1.it/fisica/sites/default/files/DOTT_FISICA/MENU/03DOTTORANDI/TesiFin22/Biccari.pdf.